

Dislocation polarization and space-charge relaxation in solid solutions $Ba_{1-x}La_xF_{2+x}$

E. Laredo, N. Suarez, A. Bello, M. Puma, and D. Figueroa

Department of Physics, Universidad Simon Bolivar, P.O. Box 80659, Caracas 1080-A, Venezuela

J. Schoonman

Department of Inorganic Chemistry, Delft University of Technology, P.O. Box 5045, 2600 Delft, The Netherlands

(Received 29 July 1985)

Concentrated solid solutions $Ba_{1-x}La_xF_{2+x}$, $x \leq 0.492$, are studied by means of thermally stimulated depolarization [ionic thermal current (ITC)] or polarization [thermally stimulated polarization current (TSPC)] techniques. At high temperature two peaks are reported whose maxima shift to lower temperatures as x increases. The energies calculated for these relaxation processes are compared to the enthalpies deduced from conductivity measurements. The first high-temperature peak, D , has been already reported in a more restricted concentration range and has been attributed to either a space-charge accumulation near the electrodes or the polarization of the dislocations present in the crystal. We show here that it is the highest-temperature peak reported here for the first time and labeled as peak E which is best related to the displacement of free interstitial fluorines through the bulk of the crystal; that is, to the building up of a space charge near the electrodes. At low concentrations the behavior of peaks D and E is understood if the Debye-Hückel interaction energy among unassociated defects is taken into account. For the more concentrated region ($x \geq 0.05$), the enhanced ionic motion model proposed to explain the variation of the ionic conductivity slopes as a function of x also applies here; the parameters present in the model are calculated and are found to be in agreement with those previously reported. The energy difference observed between peaks D and E is almost constant for $x \geq 0.05$. This energy difference equal to 0.08 eV is attributed to the binding energy of the interstitial fluorines forming the dislocation charge cloud to the dislocation line. TSPC experiments are carried out on the same crystals and they show that peak D is present in all the TSPC spectra, thus confirming the localized displacement of the charges, while the highest-temperature peak E is replaced by a steep increase of the ionic current. Therefore, the origin of peak E observed in ITC must be attributed to the accumulation of charges near the electrodes; that is, the build up of the space-charge layer.

I. INTRODUCTION

Anion excess fluorite-type solutions $Ba_{1-x}La_xF_{2+x}$ have been the subject of numerous studies since we first reported¹ the existence of an intense peak in the thermally stimulated depolarization (ITC) spectrum located at high temperature, the anomalous behavior of which deserved special attention. This first ITC study was made on crystals doped with LaF_3 up to molar fractions x of 0.01. Then, crystals with x as high as 0.492 were grown and the resulting solid solutions were studied by means of ionic conductivity,² ac dielectric loss,³ nuclear magnetic resonance⁴ of ^{19}F , neutron diffraction,⁵ and ITC.⁶ These different techniques can provide detailed information on the motion of free defects in addition to the localized motion of interstitial fluorines, F_i^- bound to a single La^{3+} , thus forming nearest-neighbor (NN) or next-nearest-neighbor (NNN) dipoles. More complicated polarizable defects, e.g., L-shaped clusters, 2:2:2 dimers,⁵ etc., can also be formed by the aggregation of simple dipolar specie.

The extension of the molar fraction up to $x=0.492$ has allowed a more thorough study of the behavior of the high-temperature (HT) part of the ITC spectrum; its complexity has caused varied interpretations related to the origin of the observed relaxations and to the transport mechanisms present in these highly doped materials.

ITC studies on crystals with a doping level $0.001 \leq x \leq 0.01$ showed¹ that the HT peak was related to the polarization of the dislocations present in the matrix; that is, the deformation of the charge cloud made of F_i^- that surrounds the dislocation line. Another way to visualize this polarization is through a Maxwell-Wagner-Sillars model for interfacial polarization. In any of these interpretations, the movement of the F_i^- under the application of the external electric field is limited and the mobile defects are weakly bound to the dislocation.

Another interpretation of the origin of this same HT peak studied in a more extended concentration range ($0.0001 \leq x \leq 0.20$) has been proposed by den Hartog.⁶ The relaxation of macroscopic space charges accumulated near the electrodes is held responsible for the HT peak. Based on the displacement in temperature of the maximum of the HT peak, a percolation-type conduction mechanism was proposed for these concentrated solid solutions. Above a critical concentration of a few atomic percent, the individual dipoles are assumed to interact strongly and a given F_i^- jumping around a La^{3+} may switch to another La^{3+} located in the vicinity.

For this same system Wapenaar *et al.*² proposed an enhanced ionic motion (EIM) to model the composition

dependence of the ionic conductivity at high concentrations and over a much wider temperature range than the one that can be explored by studying the HT peak in ITC experiments.

In this paper we will present new ITC and TSPC (thermally stimulated polarization current) results on this same system, $\text{BaF}_2:\text{La}^{3+}$, for the whole concentration range where these solid solutions exist ($x \leq 0.50$). We will focus on the high-temperature part of the spectra and discuss our results in the light of the different existing models for the transport processes in these materials.

II. THEORY

In a previous paper⁷ the expression for the depolarization current was deduced in the case of N_D dipoles per unit volume, each with a dipole moment μ , when the disorientation energy for the dipole was not considered single valued. An energy distribution around a mean value E_0 was assumed and it was shown that a Gaussian distribution of width p was the best for fitting the experimental results. With these assumptions the expression for the ITC can be written as

$$J_D(T) = \frac{1}{p\sqrt{\pi}} \int_{-\infty}^{+\infty} dE \exp\left[-\frac{(E-E_0)^2}{p^2}\right] J_D(T, E), \quad (1)$$

where

$$J_D(T, E) = \frac{P_0}{\tau_0} \exp\left[-\frac{E}{kT}\right] \exp\left[-\frac{1}{b\tau_0} \int_0^T dT' \exp\left[-\frac{E}{kT'}\right]\right],$$

$P_0 = N_D \mu^2 E_P / 3kT_P$, E_P is the electric polarizing field, T_P is the polarization temperature, b is the heating rate, and τ_0 is the inverse frequency factor.

In the same way, the polarizing current $J_P(T)$ describing the build up of the polarization in a TSPC experiment with a null initial polarization can be written as

$$J_P(T) = \frac{1}{p\sqrt{\pi}} \int_{-\infty}^{+\infty} dE \exp\left[-\frac{(E-E_0)^2}{p^2}\right] J_P(T, E), \quad (2)$$

where

$$J_P(T, E) = \frac{1}{\tau(T)} \exp\left[-\int_{T_0}^T \frac{dT'}{b\tau(T')}\right] \int_{T_0}^T dT' \left[\frac{P_0(T')}{\tau(T')} \exp\left[-\int_{T_0}^{T'} \frac{dT''}{b\tau(T'')}\right] \right] - \frac{P_0(T)}{\tau(T)},$$

and $P_0(T) = N_D \mu^2 E_P / 3kT$ and $\tau(T) = \tau_0 \exp(E/kT)$.

If the high-temperature relaxations are related to the motion of the free interstitials through the crystal, or to the carriers that are weakly bound to the dislocations, the energies involved can be related to the activation enthalpies deduced from the conductivity measurements. The EIM model² valid for the high-concentration region, $x \geq 0.05$, assumes that, due to the formation of defect clusters whose number increases with the solute content, the activation enthalpy for the mobility of the defects is not single valued, but has a Gaussian distribution of width p around a mean value $\langle \Delta H_m(x) \rangle$. The temperature dependence of the activation enthalpy can then be written as

$$\Delta H_m(T, x) = \langle \Delta H_m \rangle - p^2 / 4kT, \quad (3)$$

and it can be calculated from the slope ΔH_σ of the conductivity plots $\log_{10}(\sigma T)$ versus T^{-1} ; that is,

$$\Delta H_\sigma = \langle \Delta H_m \rangle - p^2 / 2kT. \quad (4)$$

If the concentration dependence of p and $\langle \Delta H_m \rangle$ is explicitly written, the slope of the conductivity plot varies with x according to

$$\Delta H_\sigma = \Delta H_m^0 - \left[\frac{C^2}{2kT} + h \right] x, \quad (5)$$

where C and h were estimated by Wapenaar *et al.*² and ΔH_m^0 is the true value for the free-defect migration energy found from an extrapolation to $x=0$ of $\Delta H_\sigma = f(x)$.

For a more dilute concentration range, the conductivity is influenced by the dissociation of dipoles, which increases the number of free defects as the temperature increases. The dissociation equilibrium equation then, according to Lidiard,⁸ must include the Debye-Hückel energy term, which is due to the interaction between the unassociated defects and their surrounding charge cloud. The effect of the Debye-Hückel energy results in a decrease in the slopes of the conductivity plots $\log_{10}(\sigma T) = f(1/T)$ for low values of x .

III. EXPERIMENTAL PROCEDURE

A. Crystal growth

The samples of composition $\text{Ba}_{1-x}\text{La}_x\text{F}_{2+x}$ for $x > 0.02$ were obtained from the Solid State Department of Utrecht University. The crystals were grown² by the Bridgman technique, using a rf coil to melt the mixture of powders. The crucibles employed were made of graphite and the cell was made of quartz; PbF_2 was used as a "scavenger" for any traces of oxygen or water vapor, and Merck Suprapur BaF_2 , together with 99.9%-pure Alpha Division LaF_3 , were the starting powders. The solute con-

tent of the crystals was determined by neutron-activation analysis. Neither electron-diffraction nor Debye-Scherrer techniques showed the presence of precipitates or disorder in the matrix.

B. ITC and TSPC measurements.

The measuring system is the same for the two techniques, the only difference coming from the sequence of field application and current recording. When recording the ITC spectrum, the sample is polarized at a chosen temperature, T_P , then quenched to liquid-nitrogen temperature (LN_2), where the electric field E_P is switched off. Then the temperature is raised at a constant rate, b (which in our case is $\sim 0.1 \text{ K s}^{-1}$), while the electrometer (Cary 401) records the current emitted by the sample. For the TSPC experiments we start from LN_2 temperature, and with a battery (typically, $V_P \approx 50 \text{ V}$) inserted between the electrometer and the sample we record the polarizing current (which is opposite in sign to the ITC current) as the temperature increases linearly ($b \approx 0.1 \text{ K s}^{-1}$). In both cases the cell atmosphere must be extremely clean with all traces of humidity removed by appropriate traps.

IV. RESULTS AND DISCUSSION

A. ITC experiments

The results obtained for ITC runs on solid solutions in the intermediate-concentration range are presented in Fig. 1. The polarizing temperature is 370 K, and all the curves are normalized for a unique polarizing field and crystal size. The low-temperature part of the spectrum is composed of three different peaks, *A*, *B*, and *C*, located at $T_{MA} = 115 \text{ K}$, $T_{MB} = 144 \text{ K}$, and $T_{MC} = 196 \text{ K}$, and the intensity of each peak is an increasing function of x for $x \leq 0.02$. In addition to these three peaks, the high-temperature zone shows the presence of two relaxations, *D* and *E*, whose positions shift to lower temperatures as the solute content increases. In Fig. 2 the results obtained for the ITC runs of more concentrated solid solutions are shown. In Table I we report the variation of the positions

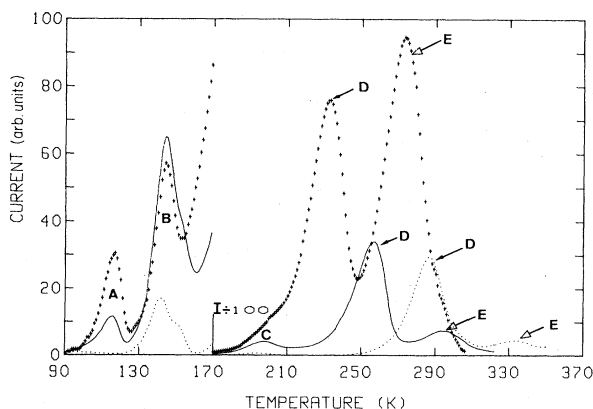


FIG. 1. ITC spectrum of $\text{Ba}_{1-x}\text{La}_x\text{F}_{2+x}$ for crystals with different molar fractions, $T_P = 370 \text{ K}$: \cdots , $x = 0.001$; --- , $x = 0.01$; $+++++$, $x = 0.0237$. The scale current is expressed in arbitrary units.

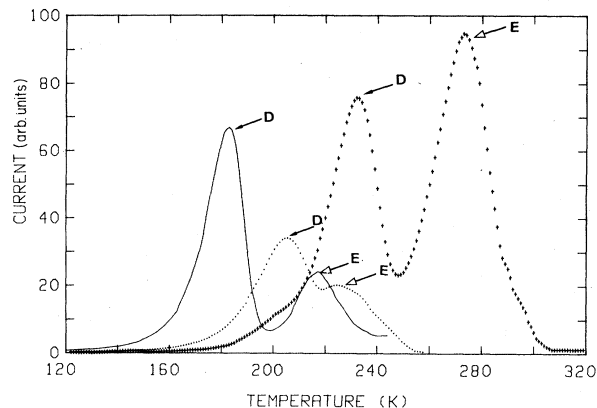


FIG. 2. ITC spectrum of $\text{Ba}_{1-x}\text{La}_x\text{F}_{2+x}$ for crystals with different molar fractions, $T_P = 370 \text{ K}$: $+++++$, $x = 0.0237$; \cdots , $x = 0.133$; --- , $x = 0.492$. The scale current is expressed in arbitrary units.

of the current maxima for peaks *E* and *D* as a function of the molar fraction x . One can observe the decrease of T_{MD} and T_{ME} with x , although the rates of change of these temperatures are much lower for concentrated crystals than for dilute ones. The existence of peak *E* at higher temperature than peak *D* and its behavior with increasing concentration is reported here for the first time. Our previous results¹ on crystals with $x \leq 0.01$ did not include peak *E* as our experiments at that time did not explore temperatures higher than 300 K. Thus, the study was restricted to peak *D* and its origin was attributed to the polarization of the dislocations, that is, a displacement of the charge cloud made of mobile F_i^- relative to the dislocation line. This assignment was based on the behavior of peak *D* after a mechanical deformation of the crystal. Its position in temperature did not change, but the peak intensity increased together with the dislocation density measured on micrographs of the surface of the sample after an attack with a dilute solution of nitric acid. The zone around the dislocations can be visualized as inclusions with a conductivity different from that of the matrix, which will result in a Maxwell-Wagner-Sillars-type polarization.

Following our previous identifications, and in agree-

TABLE I. Positions of the maximum current for peaks *E* and *D* in $\text{Ba}_{1-x}\text{La}_x\text{F}_{2+x}$, for the different molar fractions studied here.

x (molar fraction)	T_{MD} (K)	T_{ME} (K)
0.001	286.7	333.8
0.010	259.7	304.6
0.0237	232.0	273.0
0.133	204.4	222.9
0.138	212.4	235.1
0.155	201.2	230.8
0.393	192.8	219.1
0.492	182.5	217.2

ment with other authors, we assign peak *B* to the relaxation of NN dipoles and the more intense peak *C* to that of NNN dipoles, which are the more abundant species. This has been recently confirmed by the results of lattice-simulation calculations.⁹ In $\text{BaF}_2:\text{La}^{3+}$ the energy change upon substituting a La^{3+} ion for the host cation to form a NNN dipole is larger than that to form a NN dipole (-0.546 and -0.423 eV, respectively).

Peak *A*, which appears only for intermediate values of x , can be due to a small cluster such as the L-shaped $\text{La}^{3+}\text{-F}_{i2}^-$ which is formed by the trapping of a free fluorine interstitial at an existing dipole. The defect simulation⁹ for the formation of these types of defects shows that both the linear and bent complexes formed by the addition of an interstitial fluorine to an NNN dipole are probable as the estimated energy changes are negative. However, it is worth noting that peak *A* is located at 115 K, which is the zone where we have found a peak that we have attributed to oxygen dipoles in $\text{SrF}_2:\text{La}^{3+}$. When the samples were oxidized at 1100 K, a narrow peak appeared at this temperature and its intensity increased with oxidizing time. Furthermore, quenchings or annealings of the oxidized crystal left this peak unchanged. In this case we attributed this relaxation to simple dipolar $\text{O}^{2-}\text{-F}_v^-$ species, and this could also be the origin of peak *A* in BaF_2 . The intensity dependence on the concentration of these low-temperature peaks cannot be followed quantitatively for the whole concentration range. This is due to the fact that for x as low as 0.0237 the overlap with peak *D*, which is moving to lower temperature, is already significant. It is to be noted that the position of the maximum current of peak *D* for $x=0.492$ ($T_{MD}=183$ K) is located at a temperature lower than the position of the NNN dipolar peak ($T_{MC}=196$ K). Values published by den Hartog *et al.*⁶ for the maximum current temperature for his high-temperature peak are in excellent agreement with our values of T_{MD} , thus indicating that their HT peak is the same as our peak *D*. These same authors, who studied crystals with $x \leq 0.20$, state that the HT peak stops shifting to lower temperatures when the position of the NNN peak is reached. Their model assumes that the NNN dipole is the responsible specie for the percolation mechanism. The existence for higher concentrations of peak *D* at temperatures below T_{MC} indicates that the NNN dipole is not what originates the percolation process. In the wide concentration range studied here, no relation between the molar fraction x and the intensities of peaks *D* and *E* could be found, thus indicating that the processes responsible for these relaxations are not directly related to the doping level of the sample. Furthermore, the crystal surface quality, the dislocation density, and the thermal history of the sample influence the intensity of these peaks.

In an attempt to transform the positions of the HT peaks to activation enthalpies that can be compared to the values deduced from conductivity slopes, we assume that the shifting to lower temperatures can be accounted for by a variation in the energy involved in the dipolar relaxations exclusively. The inverse frequency factor τ_0 is kept constant and equal to 2.5×10^{-14} s for both peaks *D* and *E*. Wapenaar *et al.*³ measured for τ_0^Σ , which is the inverse frequency factor of their high-temperature relaxa-

tion labeled Σ , values between 10^{-15} and 10^{-14} s. This estimate was made after dielectric-loss experiments by plotting $\log_{10}(\tau_M)$ versus T^{-1} . The variation of $T_M=f(x)$ is then observed in Fig. 3 as a variation in activation energies involved in the relaxation of peaks *D* and *E*. In this figure we have also reported the values of ΔH_σ measured from the slopes of the conductivity plots by Wapenaar *et al.*² for the same crystals used in the present work. This dependence of the conductivity activation enthalpies as a function of x has been confirmed more recently by Fedorov *et al.*¹⁰ A striking similarity between energy values deduced from conductivity slopes and energy values determined from the relaxations *D* and *E* is evident in Fig. 3. This was to be expected, as the high-temperature peaks are related either to the displacement of mobile charges that can be restricted to a zone around the dislocations, or to free interstitials moving through the bulk of the crystal.

More exact values for the reorientation energies would have been obtained if these high-temperature curves were suitable for the computer fitting that we usually perform on ITC peaks. Unfortunately, several attempts to fit these curves to a model which includes a Gaussian distribution of energies failed. One reason for this failure is the difficulty involved in efficiently cleaning⁷ these peaks. One possible way to estimate the energy values was from the observed T_M and assuming a constant value for τ_0 . In doing so we arrive at some interesting results. First, we observe that for $x=0$ both ΔH_σ measured from the conductivity slopes and the energies estimated for peak *E* extrapolate at 0.717 eV, which agrees very well with the value of 0.72 eV for the migration energy of interstitial fluorines determined by Jacobs and Ong¹¹ from computer fitting of ionic conductivity data of BaF_2 doped with La^{3+} , Na^+ , and K^+ . This result is a first indication that the process responsible for peak *E* is similar to the one involved for the migration of free interstitial fluorines, which is measured by ionic conductivity. That is, peak *E*

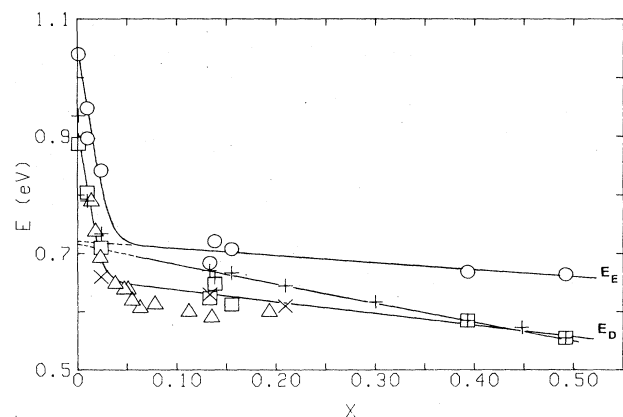


FIG. 3. The dependence of the reorientation energies on the La^{3+} molar fraction x calculated from the position of the maximum current: \square — \square — \square — for peak *D*, \circ — \circ — \circ — for peak *E*; Δ for the HT peak (Ref. 6), $+$ for ΔH_σ deduced from ionic conductivity (Ref. 2) and for ΔH^Σ from dielectric-loss experiments (Ref. 3).

originates by the migration of free interstitials which tend to accumulate near the positive electrode.

In the dilute zone, in order to explain the steep decrease of the enthalpy measured by both ITC and conductivity methods, the Debye-Hückel interaction ΔH_{DH} of unassociated defects must be considered. Lidiard⁸ has shown that for moderate dopant concentration the ideal-solution approximation must be modified to include the screening due to the charge cloud surrounding the free defect. This effect reduces both the mobility and the association energy ΔH_a of the dipole, thus resulting in a steep decrease of the conductivity slopes ΔH_σ , which in the low-temperature zone can be written as

$$\Delta H_\sigma = \Delta H_m + \frac{1}{2}(\Delta H_a - \Delta H_{DH}) . \quad (6)$$

This Debye-Hückel term, whose magnitude increases with x in the low- to intermediate-concentration range, is adequate to account for the observed decrease in the conductivity slopes, and gives a value for the association enthalpy in agreement with that calculated² for the NNN dipole (0.39 eV). A similar behavior is observed for the energies related to ITC peaks D and E and the same argument given above applies. As peak D originates from the migration of the F_i^- which are weakly bound to the dislocations, forming a mobile charge cloud, the energies involved in this relaxation must change in the low- to intermediate-concentration range in a similar manner as ΔH_σ due to the Debye-Hückel effect. For peak E attributed to the free-interstitial motion through the bulk, the effect of the Debye-Hückel energy contribution should also decrease the energy necessary for the relaxation of the space-charge layer. The difference between the energies of peaks D and E is easily understood if we consider the binding energy of the interstitial fluorine to the dislocation lines, which will further decrease the calculated energy for the relaxation of peak D .

When we reach the concentration region, $x \geq 0.05$, the picture changes as the decrease of the energies of peaks D and E is much less dramatic than for smaller concentrations. The two lines shown in Fig. 3 are almost parallel; the difference of 0.08 eV between the two lines is an estimate of the mean binding energy of the interstitial fluorines that form the dislocation charge cloud bound to the dislocation line.

Another difference can be observed between the energy ΔH_σ , deduced from conductivity slopes, and the energies determined from the positions of the maximum current of the two high-temperature ITC peaks. The three of them hold a linear relation with x . The energies of the conductivity plots are intermediate among those of peaks D and E . In the EIM model² the conductivity activation enthalpy ΔH_σ is described by relation (4). The width of the Gaussian distribution, if it is due to the monopole-monopole interaction p_{m-m} , is proportional to the square root of the monopole concentration x_m , which, in turn, is proportional to the total concentration x . This monopole-monopole interaction between free interstitial fluorine accounts entirely for the linear decrease of ΔH_σ with x if $\langle \Delta H_m \rangle$, the mean value of the Gaussian energy distribution, is considered fixed. Since in fluorites the reorientation energies for dipoles are always lower than

the free migration enthalpies in the undisturbed lattice, ΔH_m^0 , Wapenaar *et al.*² included in their model a linear decrease of $\langle \Delta H_m \rangle$ with x . Finally, the slope of the conductivity in this region can be written as in relation (5).

The values of $h=0.20$ eV and $C^2/2kT=0.13$ eV for an average measuring temperature of 450 K were estimated from the conductivity results reported² after an analysis of the dependence of $\log_{10}(\sigma T)$ on ΔH_σ . Owing to the assumptions we have made in order to convert the peak temperatures T_{MD} and T_{ME} to E_D and E_E , respectively, we have not taken into account the fact that the energy is not unique and that it has a Gaussian distribution around a mean value. Thus, the difference between E_E and ΔH_σ is a direct measure of the corrective term in expression (4), which is proportional to x and is due to the width of the distribution.

The variation of E_E , expressed in eV, with x can be written

$$E_E = 0.721 - 0.12x ,$$

to be compared to

$$\Delta H_\sigma = 0.714 - 0.33x .$$

From the difference of the two curves E_E and ΔH_σ versus x in Fig. 3, the dependence of p_{m-m} in eV as a function of x is found to be

$$p_{m-m} = 0.13\sqrt{x} .$$

The proportionality factor between p_{m-m} and $x^{1/2}$ calculated here is in good agreement with that of Wapenaar *et al.*,² who found a proportionality factor of 0.1 instead of 0.13 eV. The values of p found in this way are what one expects based on our experience of fitting curves to a Gaussian distribution of energies in a more dilute concentration range.¹² From the linear dependence of E_E with x , which can now be attributed to the variation of $\langle \Delta H_m \rangle$ with x , we can calculate a value of 0.12 eV for h ; this is somewhat smaller than the value of 0.20 eV found by Wapenaar *et al.*,² which was deduced from the variation of $\log_{10}(\sigma T)$ versus ΔH_σ in a temperature range from 333 to 500 K. The remarkable quantitative agreement between our values with those calculated by Wapenaar *et al.*² for the parameters that are defined in the EIM model shows that our initial assumptions are adequately justified. The origin of peak E identified as the relaxation of a macroscopic space charge is thus confirmed. Peak D which has been sometimes erroneously attributed to this process is now more likely to be assigned to a more localized motion of the free carriers.

B. TSPC experiments

In Figs. 4 and 5 we present the TSPC spectra corresponding to the crystals whose ITC spectra are shown in Figs. 1 and 2. The low-temperature zone shows no difference with the ITC peaks, even when drawn on a very sensitive scale, as the expected current reversal on the high-temperature tail of the TSPC peaks is present also in the ITC spectrum polarized at high temperatures, as we have reported in detail elsewhere.¹³ At higher temperatures a peak which is located at the same temperature as peak D

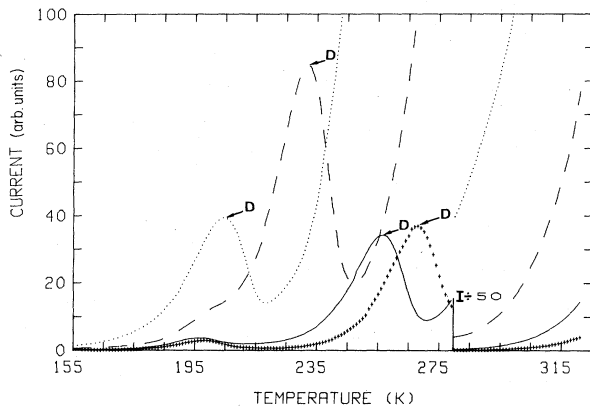


FIG. 4. TSPC spectrum of $\text{Ba}_{1-x}\text{La}_x\text{F}_{2+x}$ for crystals with different molar fractions: + + + + +, $x=0.005$; —, $x=0.01$; - - -, $x=0.0237$; . . . , $x=0.133$. The scale current is expressed in arbitrary units and is opposite in sign to the ITC current.

in the ITC spectra shows the same shift to lower temperatures when x increases. Beyond peak D a steep increase in the current due to the ionic conductivity of the sample is observed in the region where peak E occurs in the ITC spectrum. A comparison between the two kinds of experiments allows one to distinguish between localized phenomena, such as the dipolar relaxations due to the reorientation of NN and NNN dipoles, or to small polarizable clusters, or the relative displacement of the charge cloud around a dislocation and delocalized ones such as the free-interstitial-fluorine migration through the bulk of the crystal. Due to the fact that peak D is observed in both spectra, we cannot attribute it to the delocalized process that involves motion through the bulk of the crystal. Our assignment of peak D as being due to the restricted motion of the charge cloud relative to the dislocations is in total agreement with the existence of a relaxation peak in both ITC and TSPC spectra. On the other hand, peak E , which does not exist in the TSPC spectrum, is the one that must be related to the space-charge relaxation in the crystal as it is a nonlocalized motion of carriers through the bulk of the sample.

V. CONCLUSION

Our results on highly concentrated solid solutions of $\text{Ba}_{1-x}\text{La}_x\text{F}_{2+x}$ have shown a complex high-temperature spectrum which has not been reported before. There exist two high-temperature relaxations with very similar behavior in the ITC spectra; the persistence of only one of them in the TSPC spectrum of the same crystal, and the subsequent rise in the current in the zone where the

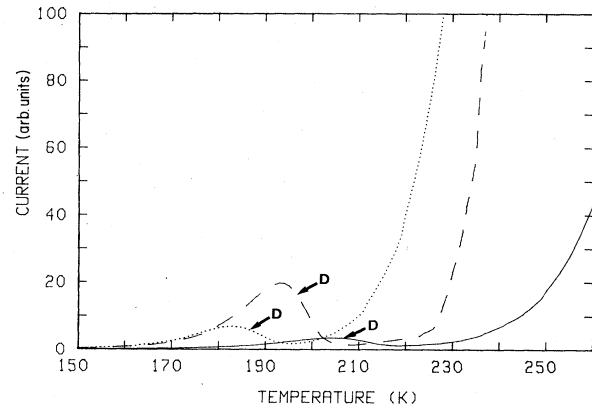


FIG. 5. TSPC spectrum of $\text{Ba}_{1-x}\text{La}_x\text{F}_{2+x}$ for crystals with different molar fractions; —, $x=0.138$; - - -, $x=0.393$; . . . , $x=0.492$. The scale current is expressed in arbitrary units and is opposite in sign to the ITC current.

highest-temperature peak was located in the ITC spectra, confirm the localized character of the relaxation process that originates peak D . This peak is the only one reported, to the best of our knowledge, by previous authors, and often attributed to space-charge accumulation. We have shown that if we transform the position of the ITC peaks to activation energies, the dependence of peak E as a function of x can be nicely explained in terms of the EIM model proposed by Wapenaar *et al.*² The two zones observed in the slopes of the ionic conductivity are reproduced here, and information about the concentration dependence of the migration energy of the free interstitial fluorine can be gathered. The values obtained for the parameters C and h of the EIM model are in excellent agreement with those previously reported² from the analysis of the conductivity results. The broadening of the energy distribution is also perfectly in line from what we know from the dilute concentration range.⁷ Thus we have established that the space-charge peak occurs in these highly concentrated solid solutions together with a lower-temperature peak which is related to the dislocations present in the crystal, in agreement with our previous assignment.¹ The energy difference between the two relaxations can be used as a measure of the binding energy of the interstitial fluorines present in the charge cloud to the dislocation lines.

ACKNOWLEDGMENT

We are deeply indebted to the Consejo Nacional de Investigaciones Científicas y Tecnológicas, which partially supported this project (CONICIT No. S1-1422).

¹E. Laredo, M. Puma, and D. R. Figueroa, *Phys. Rev. B* **19**, 2224 (1979).

²K. E. D. Wapenaar, J. L. Van Koesveld, and J. Schoonman, *Solid State Ionics* **2**, 145 (1981).

³K. E. D. Wapenaar, H. G. Koekoek, and J. Van Turnhout, *Solid State Ionics* **7**, 225 (1982).

⁴R. A. Panhuyzen, A. F. M. Arts, K. E. D. Wapenaar, and J. Schoonman, *Solid State Ionics* **5**, 641 (1981).

- ⁵J. K. Kjems, N. H. Andersen, J. Schoonman, and K. Clausen, *Physica* **120B**, 357 (1982).
- ⁶H. W. den Hartog and J. C. Langevoort, *Phys. Rev. B* **24**, 3547 (1981).
- ⁷E. Laredo, M. Puma, N. Suarez, and D. R. Figueroa, *Phys. Rev. B* **23**, 3009 (1980).
- ⁸A. B. Lidiard, in *Handbuch der Physik*, edited by S. Flügge (Springer, Berlin, 1957).
- ⁹J. Corish, C. R. A. Catlow, P. W. M. Jacobs, and S. H. Ong, *Phys. Rev. B* **25**, 6425 (1982).
- ¹⁰P. P. Fedorov, T. M. Turkina, B. P. Sobolev, E. M. Mariani, and M. Svantner, *Solid State Ionics* **6**, 331 (1982).
- ¹¹P. W. M. Jacobs and S. H. Ong, *Cryst. Lattice Defects* **8**, 177 (1980).
- ¹²E. Laredo, D. R. Figueroa, and M. Puma, *J. Phys. C* **6**, 451 (1980).
- ¹³M. Puma, A. Bello, N. Suarez, and E. Laredo, *Phys. Rev. B* **32**, 5424 (1985).